The Journal of Experimental Medicine

Growth differentiation factor 15 deficiency protects against atherosclerosis by attenuating CCR2-mediated macrophage chemotaxis

Saskia C.A. de Jager,[1] Beatriz Bermúdez,[2,8] Ilze Bot,[1] Rory R. Koenen,[3,4,8] Martine Bot,[1] Annemieke Kavelaars,[6] Vivian de Waard,[5] Cobi J. Heijnen,[6] Francisco J.G. Muriana,[2] Christian Weber,[3,4,7] Theo J.C. van Berkel,[1] Johan Kuiper,[1] Se-Jin Lee,[7] Rocio Abia,[2] and Erik A.L. Biessen[1,8]

[1]Biopharmaceutics, Leiden/Amsterdam Center for Drug Research, Leiden University, 2333CC Leiden, Netherlands
[2]Cellular and Molecular Nutrition, Instituto de la Grasa, Consejo Superior de Investigaciones Científicas, Seville 41014, Spain
[3]Institute for Molecular Cardiovascular Research, Universitäts klinikum Aachen, 52057 Aachen, Germany
[4]Institut für Prophylaxe und Epidemiologie der Kreislaufkrankheiten, Ludwig-Maximilians-Universität München, 80539 München, Germany
[5]Medical Biochemistry, Academic Medical Center, University of Amsterdam, 1105AZ Amsterdam, Netherlands
[6]Neuroimmunology and Developmental Origins of Disease, University Medical Center Utrecht, 3854EA Utrecht, Netherlands
[7]Molecular Biology and Genetics, Johns Hopkins University School of Medicine, Baltimore, MD 21205
[8]Experimental Pathology, CARIM, Academic University Hospital Maastricht, 6200MD Maastricht, Netherlands

Growth differentiation factor (GDF) 15 is a member of the transforming growth factor β (TGF–β) superfamily, which operates in acute phase responses through a currently unknown receptor. Elevated GDF–15 serum levels were recently identified as a risk factor for acute coronary syndromes. We show that GDF–15 expression is up-regulated as disease progresses in murine atherosclerosis and primarily colocalizes with plaque macrophages. Hematopoietic GDF–15 deficiency in low density lipoprotein receptor$^{-/-}$ mice led to impaired initial lesion formation and increased collagen in later lesions. Although lesion burden in GDF–15$^{-/-}$ chimeras was unaltered, plaques had reduced macrophage infiltrates and decreased necrotic core formation, all features of improved plaque stability. In vitro studies pointed to a TGFβRII–dependent regulatory role of GDF–15 in cell death regulation. Importantly, GDF–15$^{-/-}$ macrophages displayed reduced CCR2 expression, whereas GDF–15 promoted macrophage chemotaxis in a strictly CCR2– and TGFβRII–dependent manner, a phenomenon which was not observed in G protein–coupled receptor kinase 2$^{+/-}$ macrophages. In conclusion, GDF–15 deletion has a beneficial effect both in early and later atherosclerosis by inhibition of CCR2–mediated chemotaxis and by modulating cell death. Our study is the first to identify GDF–15 as an acute phase modifier of CCR2/TGFβRII–dependent inflammatory responses to vascular injury.

CORRESPONDENCE
Saskia de Jager:
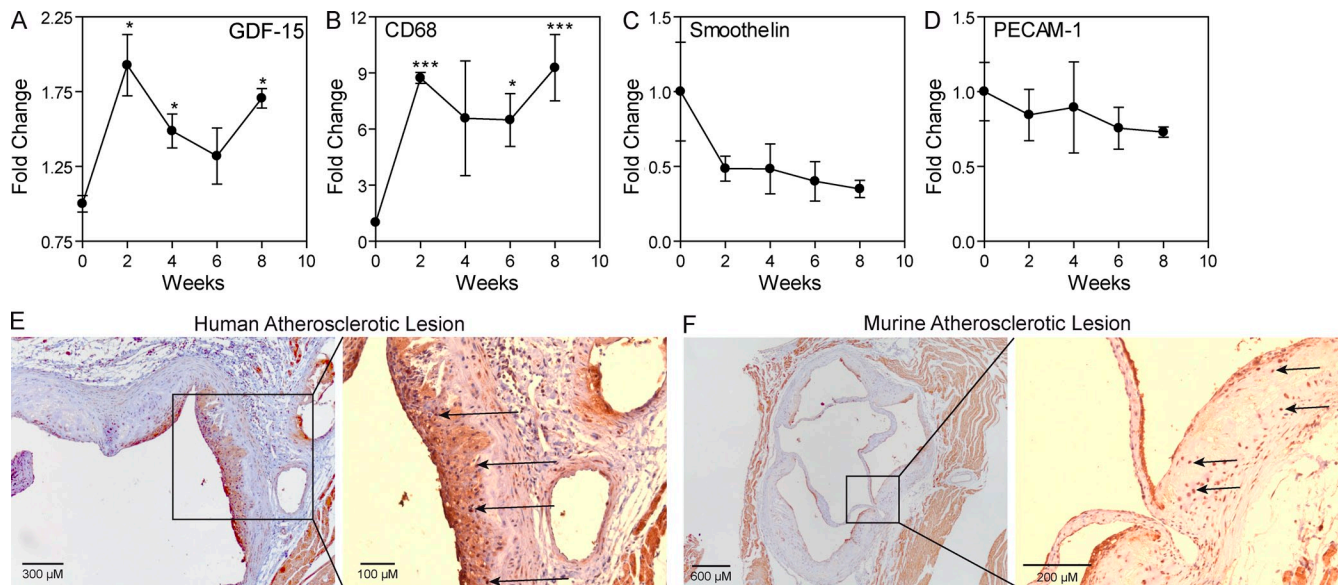s.de.jager@lacdr.leidenuniv.nl

Abbreviations used: BMP, bone morphogenic protein; CPT, camptothecin; GDF, growth differentiation factor; GRK, G protein–coupled receptor kinase; HPRT, hypoxanthine phosphoribosyl transferase; LDLr, low density lipoprotein receptor; ox-LDL, oxidized LDL; PI, propidium iodide.

The superfamily of TGF-β encompasses two major subfamilies: the TGF-β family and the bone morphogenic protein (BMP)/growth differentiation factor (GDF) subfamily (Shi and Massagué, 2003). TGF-β family members have pleiotropic effects on cell cycle (proliferation, differentiation, and apoptosis), inflammation, and cellular motility and adhesion (Massagué, 1998; Massagué et al., 2000). Generally TGF-β members interact with the common membrane-bound TGFβRII (TGF-β receptor 2), which conse-

quently forms oligomers with TGFβR1, leading to SMAD-dependent signaling (Kingsley, 1994). After nuclear translocation, SMAD complexes interact with coactivators to induce transcriptional activation of several target genes (Hogan, 1996; Liu and Niswander, 2005). Members of the BMP/GDF family interact with two serine/threonine kinase receptors (BMPR1 and BMPRII),

S.C.A. de Jager and B. Bermúdez contributed equally to this paper.

Figure 1. GDF–15 is progressively expressed in atherosclerotic lesions in a pattern similar to that of macrophages. (A–D) Temporal expression of GDF-15 (A), CD68 (B), Smoothelin (C) and PECAM-1 (D) during atherogenesis was assessed by whole genome microarray. Values are expressed as fold induction compared with time point zero. The experiment was performed twice, with $n = 3$ (each containing pooled plaque material of three mice) per time point. *, $P < 0.05$; ***, $P < 0.001$, compared with the 0-wk timepoint. Error bars are depicted as SEM. (E and F) Immunohistochemistry for GDF-15 in human (E) and murine (F) atherosclerotic lesions. Arrows represent intimal cells (based on nuclear staining) that express GDF-15.

inducing a signal transduction pathway very similar to that of the TGF-β family (Hogan, 1996; Liu and Niswander, 2005). However, BMPs were shown to have affinity for the classical TGF-β receptors and, most notably, TGFβRI as well.
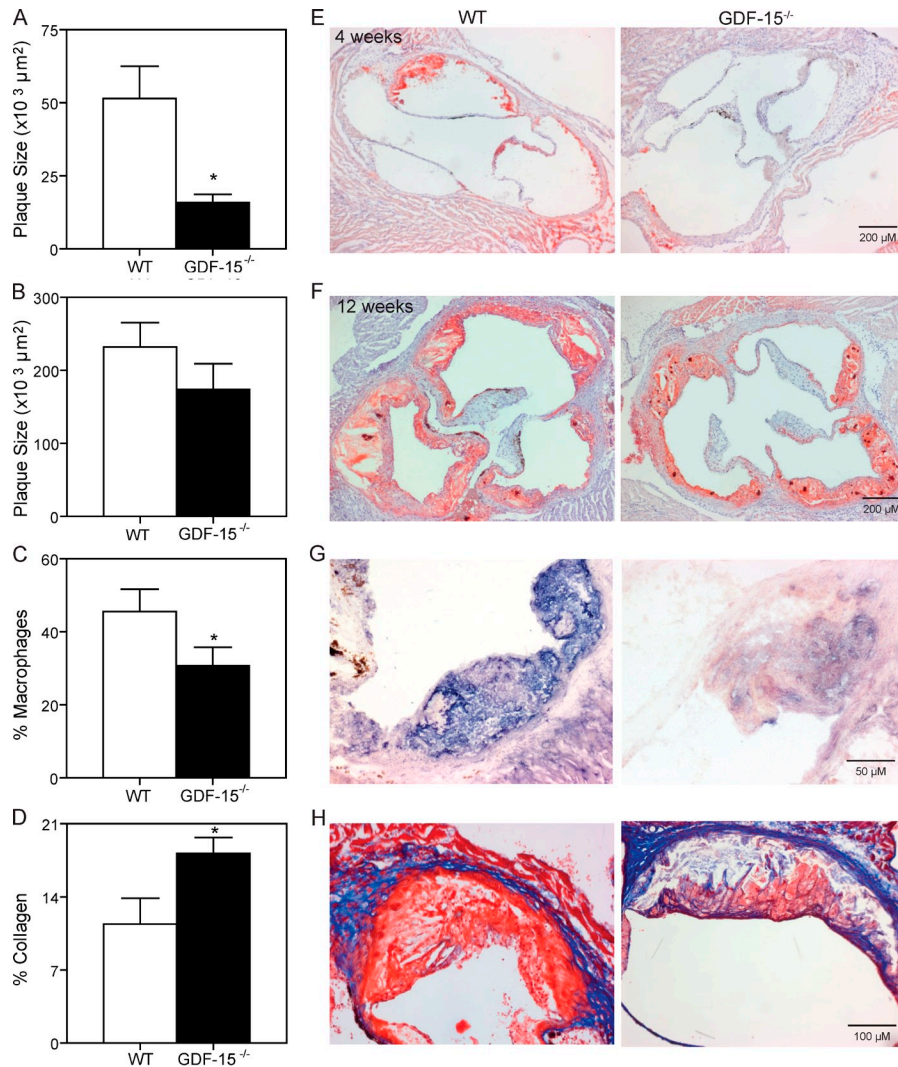
GDF-15, also known as MIC-1 (macrophage inhibitory cytokine 1), is a distant member of the subfamily of BMPs (Bootcov et al., 1997). GDF-15 has alleged antiinflammatory activity through a currently unknown receptor. It is weakly expressed under normal conditions (Bootcov et al., 1997) but is sharply up-regulated under conditions of inflammation (Hsiao et al., 2000), acting as an autocrine regulator of macrophage activation (Bootcov et al., 1997). In addition to its effects on macrophages, GDF-15 was also identified as a downstream target of p53, suggesting a role in injury response to DNA damage and in cancer.

GDF-15, both tissue-derived and circulating, appeared to be cardio-protective in mouse models for myocardial infarction and heart failure (Kempf et al., 2006; Xu et al., 2006). Paradoxically, elevated GDF-15 serum levels were shown to be an independent risk factor for early chest pain (Bouzas-Mosquera et al., 2008; Eggers et al., 2008) and acute coronary syndromes (Wollert et al., 2007; Khan et al., 2009). In this study, we have addressed the potential involvement of GDF-15 in atherogenesis, the major cause of acute cardiovascular syndromes. In this paper, we demonstrate that hematopoietic GDF-15 deficiency attenuates early lesion formation by reducing CCR2 chemotaxis and improves atherosclerotic plaque stability by enhancing collagen deposition and decreasing necrotic core expansion.

RESULTS AND DISCUSSION
GDF–15 deficiency attenuates early atherogenesis and improves plaque stability

GDF-15 is a distant member of the TGF-β superfamily (Bootcov et al., 1997), which is well known for its pleiotropic mode of action. Allelic GDF-15 mutations have been shown to associate with inflammatory disorders such as severe treatment-resistant chronic rheumatoid arthritis (Brown et al., 2007). Moreover, elevated GDF-15 serum levels are an independent risk factor for acute coronary syndromes (Wollert et al., 2007), pointing to a proatherogenic role of this cytokine. We show that GDF-15 staining mainly colocalized with subendothelial macrophages (Fig. 1 E), which concurs with earlier observations (Schlittenhardt et al., 2004). Moreover, GDF-15 expression is significantly higher (1.3-fold induced, $P = 0.0007$) in acute stages of human plaque rupture (unstable angina pectoris) than in advanced stable lesions (stable angina pectoris). GDF-15 was up-regulated in murine atherosclerotic lesions during disease progression in a pattern similar to that of the macrophage marker CD68, whereas no similarity was found with smoothelin (vascular smooth muscle cell marker) or PECAM-1 (endothelial cell marker; Fig. 1, A–D). It should, however, be noted that marker expression only reflects gross plaque expression and does not allow us to distinguish regulation of GDF-15 in individual cell types. Immunohistochemistry showed clear expression of GDF-15 in murine atherosclerotic lesions (Fig. 1 F), mainly confined to macrophage rich regions and the plaque shoulder. These findings led us to investigate the role of

Figure 2. Effects of GDF-15 deficiency on atherogenesis and plaque cellularity. Irradiated LDLr$^{-/-}$ recipients were reconstituted with WT or GDF-15$^{-/-}$ bone marrow. (A and B) Plaque size after 4 wk (A) or 12 wk (B; representative pictures in E and F). (C) Macrophages were stained with α–MoMa-2 and depicted as percentage of MoMa-2+ cells among total plaque area (representative pictures in G). (D) Collagen was visualized by Masson's trichrome staining and depicted as percentage of collagen among total plaque area (representative pictures in H). *, P < 0.05, compared with WT controls. n = 9 animals per group. The experiment was independently performed two times. Error bars are depicted as SEM.

respectively; P = 0.25; Fig. 2 B). GDF-15 deficiency apparently has a more profound impact on plaque initiation than on progression.

Despite the similar plaque size, we did notice striking differences in plaque composition between GDF-15$^{-/-}$ and WT chimeras at the 12-wk time point. Plaque cellularity was significantly decreased in GDF-15$^{-/-}$ chimeras (1.33 ± 0.11 vs. 1.94 ± 0.14 × 10^{-3} cells/μm^2 for WT; P = 0.003). This decrease was partially attributable to a decrease in plaque macrophages (30.7 ± 5.6 vs. 45.6 ± 6.1% for WT; P = 0.04; Fig. 2 C). Next to a decreased inflammatory status, plaques of GDF-15$^{-/-}$ chimeras displayed more pronounced collagen deposition (18.2 ± 1.5 in GDF-15$^{-/-}$ vs. 11.4 ± 2.5% in WT; P = 0.04; Fig. 2 D). These beneficial effects of leukocyte GDF-15 deficiency on plaque stability are in sharp contrast with that of other TGF-β family members such as activin-A (Engelse et al., 1999) and TGF-β1, where neutralization resulted in accelerated atherosclerosis and plaque destabilization (Mallat et al., 2001; Lutgens et al., 2002). Similarly, specific disruption of TGFβRII signaling aggravated atherogenesis and, again, shifted lesion composition toward a more unstable phenotype (Lutgens et al., 2002). The compositional changes observed in more advanced lesions likely reflect a decreased inflammatory status in plaques of GDF-15$^{-/-}$ chimeras resulting in a stabilized plaque phenotype. However, we cannot proclaim that the long-term composition will remain stable or perhaps progress into a more unstable phenotype during further lesion progression.

GDF-15 colocalizes with oxidized low density lipoprotein (ox-LDL) in the atherosclerotic plaque and contributes to ox-LDL induced oxidative stress and subsequent apoptosis (Schlittenhardt et al., 2004). In keeping with these findings,

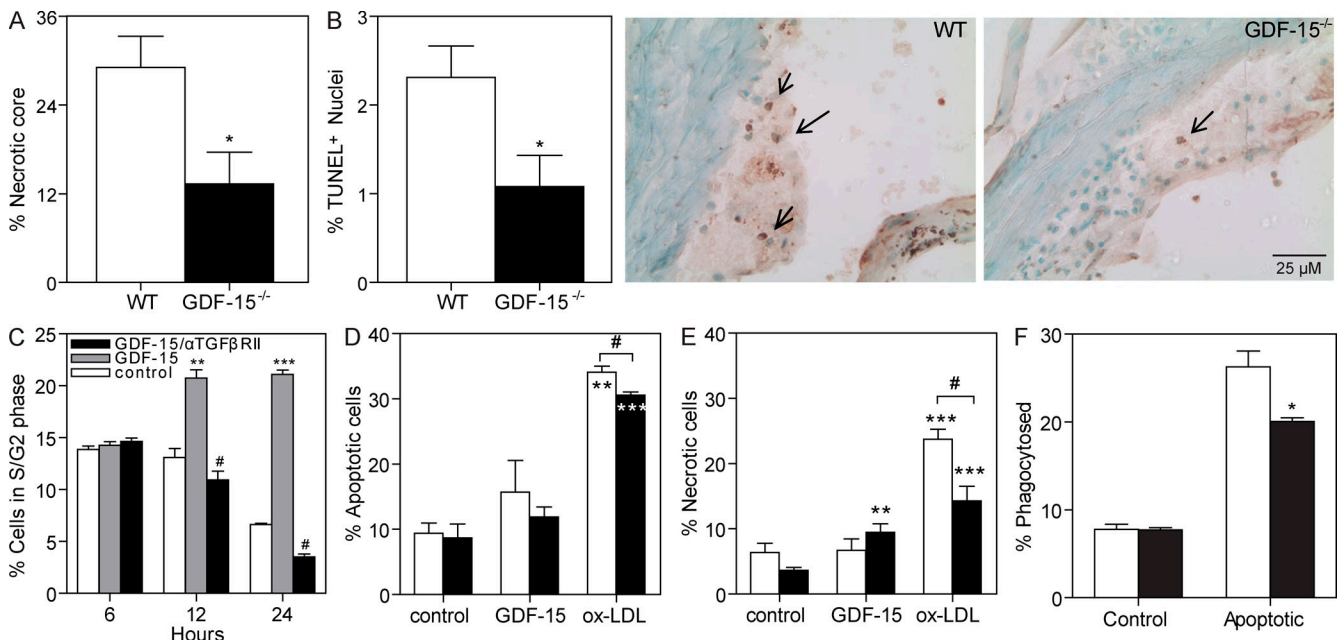leukocyte GDF-15 deficiency in atherogenesis by use of a bone marrow transplantion.

Hematopoietic GDF-15 deficiency influenced neither body weight nor total cholesterol levels throughout the experiment (unpublished data). GDF-15 expression in peritoneal macrophages and in lymphoid organs of GDF-15$^{-/-}$ chimeras was almost completely blunted, whereas GDF-15 expression in liver was reduced by a significant 60% (Table S1). Given the substantial residual hepatic GDF-15 expression, we cannot fully exclude compensatory up-regulation by nonhematopoietic sources of GDF-15 under steady-state conditions. However, as GDF-15 is mainly operational upon focal tissue injury such as in atherosclerotic tissue, we believe nonhematopoietic GDF-15 will hardly contribute to the atherogenic response.

After recovery, mice were put on a Western-type diet for 4 and 12 wk. Early lesion development (4 wk) was strongly impaired in GDF-15$^{-/-}$ chimeras (15.8 ± 2.8 in GDF-15$^{-/-}$ vs. 51.5 ± 11.0 × 10^3 μm^2 in WT chimeras; P = 0.02; Fig. 2 A), whereas at week 12 plaque burden in WT and GDF-15$^{-/-}$ chimeras was almost equalized (232 ± 33 and 174 ± 35 × 10^3 μm^2,
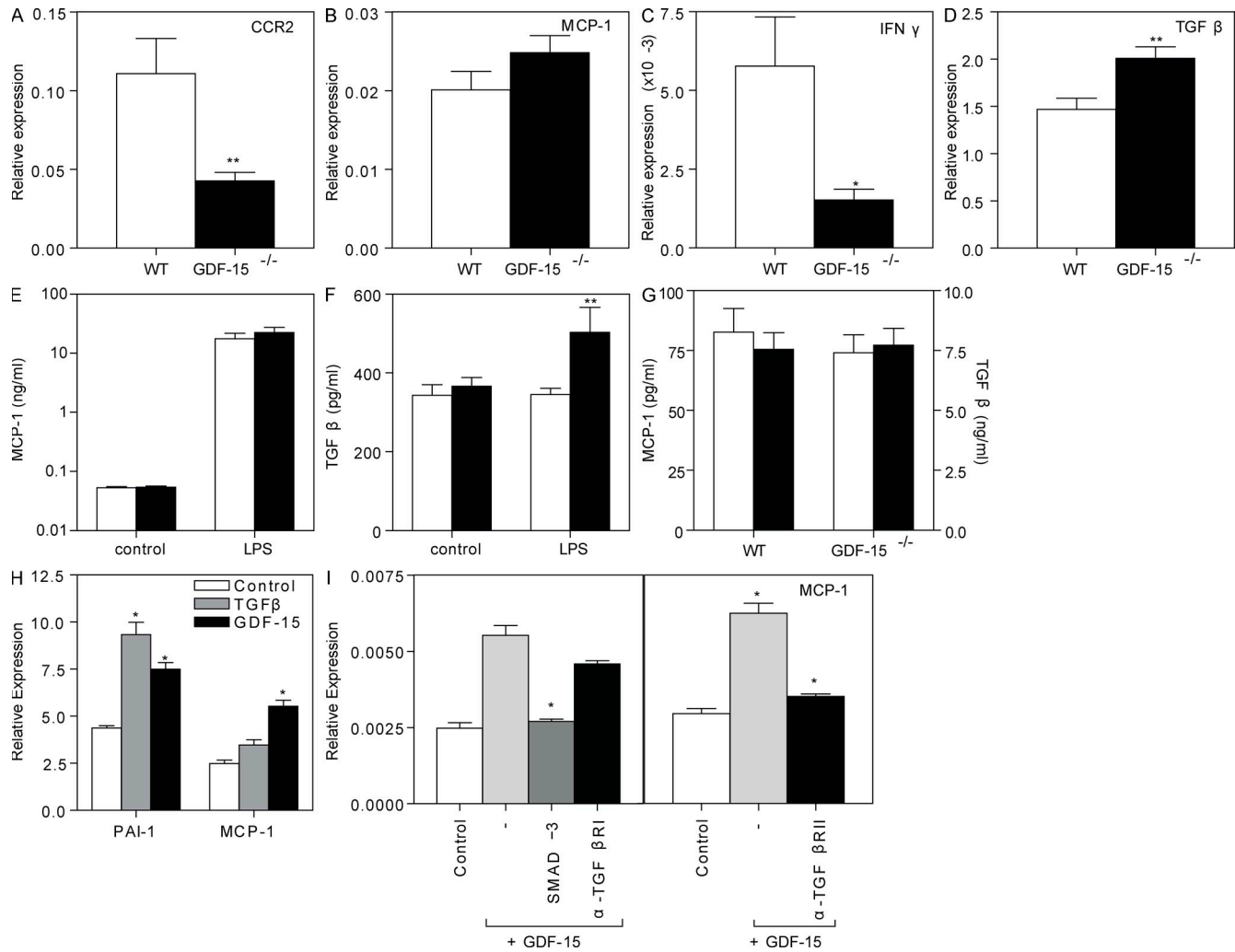
Figure 3. Effects of GDF–15 deficiency on plaque stability. (A) Necrotic core size depicted as percentage among total plaque area. (B) Cellular apoptosis was visualized by TUNEL staining and depicted as TUNEL+ cells among all mononuclear cells (including representative pictures) in week-12 plaques. *, P < 0.05, compared with WT controls (n = 9 per group). Arrows indicate TUNEL-positive nuclei. (C) S/G2 phase arrest (depicted as percentage among total cells) in RAW 264.7 macrophages after treatment with 10 ng/ml GDF-15 (gray bars) and 100 ng/ml α-TGFβRII (black bars). **, P < 0.01; ***, P < 0.001, compared with untreated controls (white bars); #, P < 0.001, compared with GDF-15 treatment. Studies were performed four times per condition and repeated in three separate experiments. (D and E) Rate of macrophage apoptosis (D; percentage annexin V+/PI− cells) and necrosis (E; percentage annexin V+/PI+ cells) after treatment with 10 ng/ml GDF-15 or 50 µg/ml ox-LDL in both GDF-15−/− (black bars) and WT (white bars) macrophages. **, P < 0.01; ***, P < 0.001 when compared with control; #, P < 0.05, compared with WT. (F) Phagocytosis capacity in WT (white bars) and GDF-15−/− (black bars) macrophages. *, P < 0.05 when compared with WT. Bone marrow–derived macrophages from WT and GDF-15 chimeras were pooled and used for apoptosis and phagocytosis assays. Each experiment was performed four times. Error bars are depicted as SEM.

we now demonstrate that the necrotic core area was significantly smaller in GDF-15−/− chimeras (13.3 ± 4.2 vs. 29.1 ± 4.2% in WT; P = 0.02; Fig. 3 A), as was the rate of intimal apoptosis (1.1 ± 0.35 vs. 2.3 ± 0.35% in WT; P = 0.03; Fig. 3 B). To further elaborate on this, we assessed whether GDF-15 was able to influence macrophage death in vitro. Exposure of RAW 264.7 macrophages to recombinant GDF-15 promoted S-to-G2 transition and did so in a TGFβRII-dependent manner (Fig. 3 C). GDF-15 did not induce apoptosis of both WT and GDF-15−/− macrophages, whereas ox-LDL and camptothecin (CPT) did so robustly (Fig. 3 D and Fig. S1 A). Ox-LDL robustly induced necrosis of WT macrophages, whereas GDF-15−/− macrophage appeared less susceptible to ox-LDL–induced necrosis (Fig. 3 E). The apoptosis inducer CPT did not influence necrosis (Fig. S1 B). Although we were unable to detect a direct effect of GDF-15 on macrophage apoptosis, our data suggest that GDF-15−/− macrophages are less susceptible to ox-LDL–induced apoptosis and necrosis (Fig. 3, D and E). Additionally, GDF-15 might have indirectly affected apoptotic cell number within the atherosclerotic plaque by affecting phagocytosis of apoptotic cells. GDF-15−/− macrophages displayed a diminished rather than increased phagocytotic capacity (24% decreased; 20.1 ± 0.4 in GDF-15−/− vs. 26.3 ± 1.8% in WT macrophages). Although it is believed

that defective clearance of apoptotic cells by macrophages leads to increased necrotic core formation and inflammation in atherosclerotic lesions (Ait-Oufella et al., 2008; Thorp et al., 2008), the minor effect on phagocytosis we observe is not likely to influence plaque inflammation and necrosis.

Hematopoietic GDF–15 deficiency does not alter monocyte differentiation and stromal release

A second striking observation was the reduced presence of macrophages in plaques of GDF-15−/− chimeras. To establish if this was a direct consequence of disturbed monocyte differentiation in these chimeras, we assessed both circulating and peritoneal monocyte numbers, which were both unaltered in the GDF-15−/− chimeras (P = 0.8 and P = 0.1; Fig. S2, A and B). As CCR2 is a crucial chemokine receptor for monocyte recruitment to early atherosclerotic lesions, we assessed the number of CCR2-expressing circulating monocytes as well. In agreement with the earlier observations, CCR2+ monocyte numbers were unaltered (P = 0.5; Fig. S2 C). To exclude the possibility that the impaired atherogenic response in GDF-15−/− chimeras is related to altered myeloid differentiation, we screened bone marrow cells by flow cytometry. CD11b+ monocyte numbers in stroma of GDF-15−/− were unchanged (P = 0.3; Fig. S2 D) and similar results were obtained for the CCR2+ monocyte
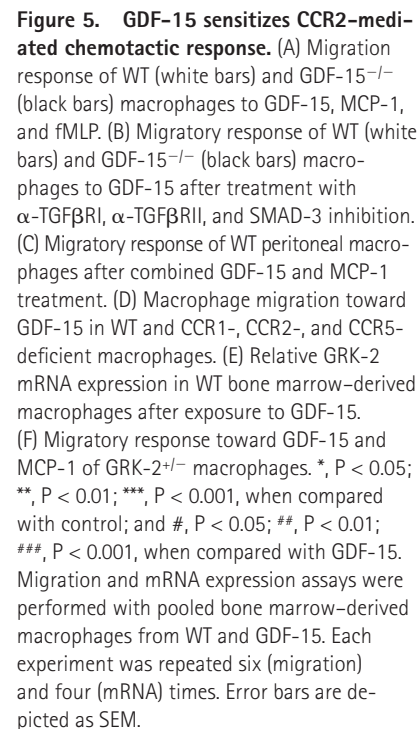
Figure 4.   Pro– and antiinflammatory mediators in GDF–15⁻ᐟ⁻ cells and chimeras. (A–D) Relative mRNA expression of CCR2 (A), MCP-1 (B), IFN-γ (C), and TGF-β (D) in WT (white bars) and GDF-15⁻ᐟ⁻ (black bars) macrophages. Values are expressed relative to average expression of GAPDH and HPRT reference genes. (E and F) MCP-1 (E) and TGF-β (F) production in WT (white bars) and GDF-15⁻ᐟ⁻ (black bars) macrophages after LPS treatment. (G) Basal levels of MCP-1 (white bars) and TGF-β (black bars) in WT and GDF-15⁻ᐟ⁻ chimeras after 4 wk of Western type diet. (H) Relative mRNA expression of PAI-1 and MCP-1 in response to 10 ng/ml GDF-15– and 15 ng/ml TGF-β1–treated WT macrophages. (I) Relative MCP-1 mRNA expression after SMAD-3 inhibition (SIS3; 3 µM) and α-TGFβRI and α-TGFβRII treatment (100 ng/ml) in WT macrophages. Bone marrow–derived macrophages from WT and GDF-15 were pooled and used for RNA expression. Each experiment was done four times. *, P < 0.05; **, P < 0.01. Error bars are depicted as SEM.

subset (P = 0.5; Fig. S2 E). GDF-15 deficiency did not skew monocyte polarization (Fig. S2 F) toward the Ly6Cʰⁱᵍʰ CCR2⁺ CX3CR1ᵐⁱᵈ phenotype, the main subset to accumulate in atherosclerotic plaques in early atherogenesis (Tacke et al., 2007). Collectively, our data suggest that stromal retention of CCR2⁺ monocytes or monocyte differentiation is not notably altered in GDF-15⁻ᐟ⁻ chimeric mice.

GDF–15–deficient macrophages display decreased CCR2 expression, accompanied by modified inflammatory characteristics
To further assess the effect of GDF-15 deficiency on macrophage characteristics, we quantified the expression of pro- and antiinflammatory mediators in macrophages from WT and GDF-15⁻ᐟ⁻ chimeras. Peritoneal macrophages were analyzed

for mRNA expression of CCR2, MCP-1, IFN-γ, and TGF-β. Interestingly GDF-15⁻ᐟ⁻ macrophages displayed decreased CCR2 expression (Fig. 4 A), whereas expression of its ligand MCP-1 was not altered (Fig. 4 B). This finding further substantiates the notion that GDF-15 mainly acts focally, as systemic inhibition of CCR2 signaling was shown to increase circulating MCP-1 levels (Vergunst et al., 2008). Additionally, membrane-expressed CCR2, but not CCR5, was up-regulated on peritoneal leukocytes upon GDF-15 exposure (Fig. S3, A and B). Basal expression of the proinflammatory cytokine IFN-γ (Fig. 4 C) was significantly down-regulated in GDF-15⁻ᐟ⁻ macrophages, whereas expression of TGF-β was increased (Fig. 4 D), reflective of antiinflammatory properties of GDF-15⁻ᐟ⁻ macrophages. In agreement with the latter, ex vivo stimulation of peritoneal GDF-15⁻ᐟ⁻ macrophages with the TLR-4 ligand

221

Figure 5. GDF-15 sensitizes CCR2-mediated chemotactic response. (A) Migration response of WT (white bars) and GDF-15$^{-/-}$ (black bars) macrophages to GDF-15, MCP-1, and fMLP. (B) Migratory response of WT (white bars) and GDF-15$^{-/-}$ (black bars) macrophages to GDF-15 after treatment with α-TGFβRI, α-TGFβRII, and SMAD-3 inhibition. (C) Migratory response of WT peritoneal macrophages after combined GDF-15 and MCP-1 treatment. (D) Macrophage migration toward GDF-15 in WT and CCR1-, CCR2-, and CCR5-deficient macrophages. (E) Relative GRK-2 mRNA expression in WT bone marrow–derived macrophages after exposure to GDF-15. (F) Migratory response toward GDF-15 and MCP-1 of GRK-2$^{+/-}$ macrophages. *, P < 0.05; **, P < 0.01; ***, P < 0.001, when compared with control; and #, P < 0.05; ##, P < 0.01; ###, P < 0.001, when compared with GDF-15. Migration and mRNA expression assays were performed with pooled bone marrow–derived macrophages from WT and GDF-15. Each experiment was repeated six (migration) and four (mRNA) times. Error bars are depicted as SEM.

LPS did not alter MCP-1 production (Fig. 4 E), but it did result in increased production of TGF-β compared with stimulated WT macrophages (Fig. 4 F). Moreover MCP-1 and TGF-β serum levels did not differ between GDF-15 and WT chimeras (Fig. 4 G), suggesting that GDF-15 may exert its immuno-modulatory effects not at a systemic but at a focal level within the plaque. The decreased inflammatory status of GDF-15$^{-/-}$ macrophages findings nicely reflect the effects on plaque stability we observed in the GDF-15$^{-/-}$ chimeras. The anti-inflammatory effects of GDF-15$^{-/-}$ macrophages directly alter intimal macrophage accumulation, apoptosis/necrosis, and collagen production, consequently resulting in distinct compositional differences of the atherosclerotic plaques (Fig. 2).

GDF-15, but not TGF-β, specifically up-regulates MCP-1 expression

As a TGF-β family member, GDF-15 is likely to signal through TGFβRII. Indeed recombinant GDF-15 and TGF-β1 were both seen to induce the expression of plasminogen activator inhibitor 1, an established TGF-β responsive gene, in RAW 264.7 macrophages (Fig. 4 H). This implies that signal transduction cascades for both cytokines partly overlap. Unlike TGF-β1, however, GDF-15 did induce MCP-1 expression (Fig. 4 B). This effect could be prevented by coincubation with a SMAD3 inhibitor, implicating this adaptor protein in GDF-15 signaling (Fig. 4 I). Blockade of TGFβRII, but not TGFβRI/ALK5, abrogated the GDF-15–elicited MCP-1 response (Fig. 4 I). This suggests that GDF-15 signaling in macrophages does not require TGFβRI; however, we cannot exclude the involvement of other ALK family members. These data demonstrate that although TGF-β and GDF-15 both signal via TGFβRII, only GDF-15 was capable of inducing MCP-1.

Hematopoietic GDF-15 deficiency attenuates MCP-1–directed macrophage migration

The findings in the previous section suggest that the reduced macrophage accumulation in plaques of GDF-15$^{-/-}$ chimeras may well be related to an impaired mobility, possibly via modulation of CCR2 function, as we observed decreased CCR2 expression on GDF-15$^{-/-}$ macrophages. This notion derives further support from the fact that, like MCP-1 (Guo et al., 2003, 2005), GDF-15 deficiency also seems to preferentially affect plaque initiation. Indeed, basal GDF-15$^{-/-}$ macrophage mobility was significantly lower than that of WT cells (Fig. S3 C). Conversely, GDF-15$^{-/-}$ cells displayed an equally potent migratory response toward GDF-15, MCP-1, or fMLP as WT macrophages (Fig. 5 A). Interestingly, GDF-15–induced migration is depended on TGFβRII and SMAD-3 signaling, whereas blockade of TGFβRI slightly potentiates GDF-15–induced migration in WT macrophages (Fig. 5 B). GDF-15 was almost equally effective at promoting macrophage migration as MCP-1 in a chemotaxis assay (Fig. 5 C). Co-stimulation of macrophages with GDF-15 and MCP-1 did not lead to an augmented response, which is suggestive of convergent migratory pathways (Fig. 5 C). To dissect interference of GDF-15 with CCR2 chemotaxis, we studied the chemotactic response of CCR1-, CCR2-, and CCR5-deficient macrophages to GDF-15. Surprisingly, GDF-15 was unable to induce CCR2$^{-/-}$ cell migration, whereas GDF-15–induced chemotaxis of CCR1$^{-/-}$ and CCR5$^{-/-}$ macrophages was unaltered (Fig. 5 D). Although these findings point to a direct interaction of GDF-15 with chemokine receptor CCR2 function, MCP-1 release by WT and GDF-15–deficient macrophages in response to LPS was essentially similar. This suggests that GDF-15–induced macrophage mobility may, at least in part, be exerted by a modulating effect of this cytokine on CCR2 responsiveness.

The activity of most G protein–coupled receptors, including CCR2, is regulated not only at the mRNA and protein

but also at the functional level via dedicated G protein–coupled receptor kinases (Vroon et al., 2006). G protein–coupled receptor kinase (GRK) 2 was reported to phosphorylate CCR2, resulting in ligand uncoupling, CCR2 internalization, and subsequent loss of CCR2 function (Aragay et al., 1998). It is of note that Ho et al. (2005) have recently identified GRK-2 as a downstream target of TGF-β that terminates TGF-β–induced Smad signaling in a negative-feedback mechanism. Thus, we argued that GDF-15 may interfere with CCR2 chemotaxis in a GRK-2–dependent manner. Exposure of macrophages to GDF-15 for 24 h indeed led to a substantial down-regulation of GRK-2 mRNA expression in WT macrophages, thereby possibly potentiating CCR2-dependent migratory responses (Fig. 5 E). Next, we assessed GDF-15–induced macrophage migration in GRK-2$^{+/-}$ macrophages. Similar to WT macrophages, MCP-1 also induced migration of GRK-2$^{+/-}$ macrophages (Fig. 5 F). In contrast, GDF-15 was unable to induce a significant migratory response in GRK-2$^{+/-}$ cells that have 50% lower GRK-2 protein expression (Fig. 5 E). Apparently GDF-15–induced macrophage migration essentially requires intact GRK-2 function and thereby possibly modulates CCR2-mediated migratory responses.

In conclusion, we are the first to demonstrate that leukocyte deficiency of GDF-15 improves atherosclerotic plaque stability by impairing macrophage migration and inducing collagen deposition. Our data not only indicate that GDF-15 and TGF-β signaling in macrophages partly overlap but also that GDF-15 dampens TGF-β function. Next to its modulatory effect on TGF-β signaling, our studies unveil a novel function for GDF-15 in the regulation of CCR2-dependent macrophage chemotaxis. Its chemotactic capacity is shown to proceed via TGFβRII and its downstream effector GRK-2 and is likely relevant to GDF-15–mediated acute phase responses. In the context of atherosclerosis, GDF-15 deficiency acts protectively by affecting two major processes as it attenuates TGF-β1 signaling and, more importantly, it amplifies CCR2-dependent macrophage migration to and accumulation in the atherosclerotic lesion.

MATERIALS AND METHODS

Animals. LDL receptor (LDLr)$^{-/-}$ and CCR2$^{-/-}$ mice (on C57BL/6 background) were obtained from the local animal breeding facility. GDF-15$^{-/-}$ and WT controls were obtained from Johns Hopkins University School of Medicine. CCR1$^{-/-}$ and CCR5$^{-/-}$ mice were obtained from University Medical Center Aachen and GRK-2$^{+/-}$ mice were obtained from the University Medical Center Utrecht animal facility. In vivo experiments were performed at the animal facilities of the Gorlaeus laboratories. All experimental protocols were approved by the ethics committee for animal experiments of Leiden University.

Bone marrow transplantation. To induce bone marrow aplasia, male LDLr$^{-/-}$ recipient mice were exposed to a single dose of 9 Gy (0.19 Gy/min, 200 kV, 4 mA) total body irradiation using an Andrex Smart 225 Röntgen source (YXLON International) with a 6-mm aluminum filter 1 d before the transplantation. Bone marrow was isolated by flushing the femurs and tibias of GDF-15$^{-/-}$ and WT mice with PBS. Subsequently, the cell suspension was gently filtered through a 70-μm cell strainer to obtain a single cell suspension (BD). Irradiated recipients received 0.5 × 10^7 bone

marrow cells by tail vein injection and were allowed to recover for 6 wk. Drinking water was supplied with antibiotics (83 mg/liter ciprofloxacin and 67 mg/liter polymyxin B sulfate) and 6.5 g/liter sucrose and provided ad libitum. Animals were placed on a Western-type diet containing 0.25% cholesterol and 15% cacao butter (SDS) diet for 4 and 12 wk and subsequently sacrificed.

Histological analysis. 10-μm cryostat sections of the aortic root were collected and stained with Oil-red-O to determine lesion size. Macrophages were visualized immunohistochemically with an antibody directed against a macrophage-specific antigen (MOMA-2, monoclonal rat IgG2b, dilution 1:50; AbD Serotec). Goat anti–rat IgG-AP (dilution 1:100; Sigma-Aldrich) was used as secondary antibody and NBT-BCIP (Dako) as enzyme substrates. Masson's trichrome staining (Sigma-Aldrich) was used to visualize collagen (blue staining). Cellular apoptosis was visualized using a terminal deoxytransferase dUTP nick-end labeling (TUNEL) kit (Roche). Apoptotic nuclei were scored manually. Intimal necrosis was determined by assessment of necrotic area in TUNEL-stained sections. Histological analysis was performed by an independent operator (SdJ).

Flow cytometry. Peritoneal leukocytes were harvested by peritoneal cavity lavage with PBS. Cells were centrifuged for 5 min at 1,500 rpm and resuspended in lysis buffer to remove residual erythrocytes. Cell suspensions were incubated with 1% normal mouse serum in PBS and stained for the surface markers F4/80 antigen, CD11b (eBioscience), Ly6C (BD), and CCR2 (clone E68; Abcam) at a concentration of 0.25 μg of antibody per 200,000 cells. Subsequently cells were subjected to flow cytometric analysis (FACSCalibur; BD). FACS data were analyzed with CellQuest software (BD).

Cell cycle. Serum-deprived RAW 264.7 macrophages were stimulated with 10 ng/ml of recombinant GDF-15 and 100 ng/ml of recombinant mouse TGFβRII/mouse FC (R&D Systems) for 6, 12, and 24 h. Cells were washed twice in PBS and fixed in ice-cold 70% ethanol for 24 h. Cells were then washed twice in HBSS and resuspended in PBS containing 0.1 mM EDTA, 0.1% Triton X-100, 50 μg/ml RNase A, and 50 μg/ml propidium iodide (PI). After incubation at room temperature for 30 min, cells were analyzed for cell cycle distribution with an EPICS XL flow cytometer (Beckman Coulter) and EXPO32 software (Beckman Coulter).

Apoptosis assay. Cellular apoptosis was measured using an Annexin V-FITC/PI staining kit (Invitrogen). Serum-deprived cells were stimulated with 10 ng/ml of recombinant GDF-15, 50 μg/ml ox-LDL, and 0.5 and 1 μM CPT (Sigma-Aldrich).

Phagocytosis assay. After induction of apoptosis of Jurkat T cells with 1 μM CPT, cells were washed two times in PBS and then labeled with 1 μg/ml CellTracker red (Invitrogen) for 1 h at 37°C at a cell concentration of 1 × 10^6 cells/ml. Fluorescently labeled apoptotic cells and macrophages were washed three times with PBS. Macrophages were incubated for 3 h at 37°C with labeled apoptotic cells (ratio of 1:5; RPMI [Invitrogen] supplemented with 10% FCS and 15% LCM). The wells were then washed two times with PBS, to remove apoptotic cells that had not been ingested. The cells were detached with 1% lidocaine (Sigma-Aldrich) in FACS (0.5% BSA/PBS) buffer and analyzed by flow cytometry.

Real-time PCR assays. mRNA levels for specific genes were determined by real-time PCR in a MX3000P system (Agilent Technologies). Reverse transcription was performed using Superscript II RT according to the manufacturer's manual. For each PCR, cDNA template was added to Brilliant SYBR green QPCR Master Mix (Agilent Technologies) containing the primer pairs for CCR2 (Forward, 5′-AGAGAGCTGCAGCAAAAAGG-3′; reverse, 5′-GGAAAGAGGCAGTTGCAAAG-3′), MCP-1(forward, 5′-AGGTCCCTGTCATGCTTCTG-3′; reverse, 5′-TCTGGACCCATT-CCTTCTTG-3′), INF-γ (forward, 5′-ACTGGCAAAAGGATGGTGAC-3′;

reverse, 5′-TGAGCTCATTGAATGCTTGG-3′), TGF-β (forward, 5′-TTGCTTCAGCTCCACAGAGA-3′; reverse, 5′-TGGTTGTAGAGGG-CAAGGAC-3′), and PAI-1 (forward, 5′-GGAGGGCACAACACTTTCAT-3′; reverse, 5′-GGCCACCATTTGATCTGTCT-3′). Primers were designed based on PRIMER3.0 (http://frodo.wi.mit.edu/primer3/input.htm). Amplification was performed in triplicate, and mean threshold cycle (Ct) numbers of the triplicates were used to calculate the relative mRNA expression of candidate genes. The magnitude of change of mRNA expression for candidate genes in RAW 267.4 was calculated using a standard curve. All data were normalized to the mean expression of endogenous reference genes (i.e., hypoxanthine phosphoribosyl transferase [HPRT] and GAPDH) and expressed as fold change over the controls.

Migration assay. Macrophages from WT, GDF-15$^{-/-}$, CCR1$^{-/-}$, CCR2$^{-/-}$, CCR5$^{-/-}$, or GRK-2$^{+/-}$ mice were cultured from bone marrow or harvested by peritoneal lavage. 10^5 macrophages were seeded onto 8-µm pore chemotaxis membranes (PAA). Medium containing the chemotactic stimuli 10 ng/ml GDF-15 (R&D Systems), 10 ng/ml of murine MCP-1 (JE; Peprotech), or 10 ng/ml of murine RANTES (Peprotech) was added to the basolateral side of the membrane and cells were allowed to migrate for 16 h. 1 nmol/liter of the chemotactic peptide fMLP (Sigma-Aldrich) was used as a positive control. The number of cells that had completely migrated to the basolateral side of the chamber was scored.

Macrophage stimulation. Serum-deprived RAW 264.7 macrophages were stimulated with 15 ng/ml of recombinant TGF-β1 or 10 ng/ml GDF-15 for 6 h. Total RNA was isolated for real-time PCR. Peritoneal macrophages were harvested by peritoneal lavage and seeded as 0.5×10^6 cells/ml. When complete cell adherence was confirmed and nonadherent cells were removed, the cells were stimulated with 100 ng/ml LPS (*Salmonella Minnesota* R595 [Re]; List Biological Laboratories Inc.) for 24 h. Subsequently, the supernatant was collected and assayed for TGF-β1 and MCP-1 levels on ELISA, according to the manufacturer's protocol (eBioscience).

Statistical analysis. Data are expressed as mean ± SEM. A two-tailed Student's *t* test was used to compare individual groups, whereas multiple groups were compared with a one-way ANOVA and a subsequent Student-Newman-Keuls multiple comparisons test. Nonparametric data were analyzed using a Mann-Whitney *U* test. A level of $P < 0.05$ was considered significant.

Online supplemental material. Fig. S1 shows effects of GDF-15 and ox-LDL on macrophage apoptosis and necrosis. Fig. S2 shows that GDF-15$^{-/-}$ chimeras display normal monocyte differentiation and release from the bone marrow. Fig. S3 shows that GDF-15 deficiency modulates CCR2 expression and responsiveness. Table S1 shows relative GDF-15 expression levels. Online supplemental material is available at http://www.jem.org/cgi/content/full/jem.20100370/DC1.

REFERENCES

Ait-Oufella, H., V. Pouresmail, T. Simon, O. Blanc-Brude, K. Kinugawa, R. Merval, G. Offenstadt, G. Lesèche, P.L. Cohen, A. Tedgui, and Z. Mallat. 2008. Defective mer receptor tyrosine kinase signaling in bone marrow cells promotes apoptotic cell accumulation and accelerates atherosclerosis. *Arterioscler. Thromb. Vasc. Biol.* 28:1429–1431. doi:10.1161/ATVBAHA.108.169078

Aragay, A.M., M. Mellado, J.M. Frade, A.M. Martin, M.C. Jimenez-Sainz, C. Martinez-A, and F. Mayor Jr. 1998. Monocyte chemoattractant protein-1-induced CCR2B receptor desensitization mediated by the G protein-coupled receptor kinase 2. *Proc. Natl. Acad. Sci. USA.* 95:2985–2990. doi:10.1073/pnas.95.6.2985

Bootcov, M.R., A.R. Bauskin, S.M. Valenzuela, A.G. Moore, M. Bansal, X.Y. He, H.P. Zhang, M. Donnellan, S. Mahler, K. Pryor, et al. 1997. MIC-1, a novel macrophage inhibitory cytokine, is a divergent member of the TGF-beta superfamily. *Proc. Natl. Acad. Sci. USA.* 94:11514–11519. doi:10.1073/pnas.94.21.11514

Bouzas-Mosquera, A., J. Peteiro, J.M. Vázquez-Rodríguez, and N. Alvarez-García. 2008. Growth-differentiation factor-15 for risk stratification in patients with acute chest pain. *Eur. Heart J.* 29:2947, author reply :2947–2948. doi:10.1093/eurheartj/ehn457

Brown, D.A., J. Moore, H. Johnen, T.J. Smeets, A.R. Bauskin, T. Kuffner, H. Weedon, S.T. Milliken, P.P. Tak, M.D. Smith, and S.N. Breit. 2007. Serum macrophage inhibitory cytokine 1 in rheumatoid arthritis: a potential marker of erosive joint destruction. *Arthritis Rheum.* 56:753–764. doi:10.1002/art.22410

Eggers, K.M., T. Kempf, T. Allhoff, B. Lindahl, L. Wallentin, and K.C. Wollert. 2008. Growth-differentiation factor-15 for early risk stratification in patients with acute chest pain. *Eur. Heart J.* 29:2327–2335. doi:10.1093/eurheartj/ehn339

Engelse, M.A., J.M. Neele, T.A. van Achterberg, B.E. van Aken, R.H. van Schaik, H. Pannekoek, and C.J. de Vries. 1999. Human activin-A is expressed in the atherosclerotic lesion and promotes the contractile phenotype of smooth muscle cells. *Circ. Res.* 85:931–939.

Guo, J., M. Van Eck, J. Twisk, N. Maeda, G.M. Benson, P.H. Groot, and T.J. Van Berkel. 2003. Transplantation of monocyte CC-chemokine receptor 2-deficient bone marrow into ApoE3-Leiden mice inhibits atherogenesis. *Arterioscler. Thromb. Vasc. Biol.* 23:447–453. doi:10.1161/01.ATV.0000058431.78833.F5

Guo, J., V. de Waard, M. Van Eck, R.B. Hildebrand, E.J. van Wanrooij, J. Kuiper, N. Maeda, G.M. Benson, P.H. Groot, and T.J. Van Berkel. 2005. Repopulation of apolipoprotein E knockout mice with CCR2-deficient bone marrow progenitor cells does not inhibit ongoing atherosclerotic lesion development. *Arterioscler. Thromb. Vasc. Biol.* 25:1014–1019. doi:10.1161/01.ATV.0000163181.40896.42

Ho, J., E. Cocolakis, V.M. Dumas, B.I. Posner, S.A. Laporte, and J.J. Lebrun. 2005. The G protein-coupled receptor kinase-2 is a TGFbeta-inducible antagonist of TGFbeta signal transduction. *EMBO J.* 24:3247–3258. doi:10.1038/sj.emboj.7600794

Hogan, B.L. 1996. Bone morphogenetic proteins in development. *Curr. Opin. Genet. Dev.* 6:432–438. doi:10.1016/S0959-437X(96)80064-5

Hsiao, E.C., L.G. Koniaris, T. Zimmers-Koniaris, S.M. Sebald, T.V. Huynh, and S.J. Lee. 2000. Characterization of growth-differentiation factor 15, a transforming growth factor beta superfamily member induced following liver injury. *Mol. Cell. Biol.* 20:3742–3751. doi:10.1128/MCB.20.10.3742-3751.2000

Kempf, T., M. Eden, J. Strelau, M. Naguib, C. Willenbockel, J. Tongers, J. Heineke, D. Kotlarz, J. Xu, J.D. Molkentin, et al. 2006. The transforming growth factor-beta superfamily member growth-differentiation factor-15 protects the heart from ischemia/reperfusion injury. *Circ. Res.* 98:351–360. doi:10.1161/01.RES.0000202805.73038.48

Khan, S.Q., K. Ng, O. Dhillon, D. Kelly, P. Quinn, I.B. Squire, J.E. Davies, and L.L. Ng. 2009. Growth differentiation factor-15 as a prognostic marker in patients with acute myocardial infarction. *Eur. Heart J.* 30:1057–1065. doi:10.1093/eurheartj/ehn600

Kingsley, D.M. 1994. The TGF-beta superfamily: new members, new receptors, and new genetic tests of function in different organisms. *Genes Dev.* 8:133–146. doi:10.1101/gad.8.2.133

Liu, A., and L.A. Niswander. 2005. Bone morphogenetic protein signalling and vertebrate nervous system development. *Nat. Rev. Neurosci.* 6:945–954. doi:10.1038/nrn1805

Lutgens, E., M. Gijbels, M. Smook, P. Heeringa, P. Gotwals, V.E. Koteliansky, and M.J. Daemen. 2002. Transforming growth factor-beta mediates balance between inflammation and fibrosis during plaque progression. *Arterioscler. Thromb. Vasc. Biol.* 22:975–982. doi:10.1161/01 .ATV.0000019729.39500.2F

Mallat, Z., A. Gojova, C. Marchiol-Fournigault, B. Esposito, C. Kamaté, R. Merval, D. Fradelizi, and A. Tedgui. 2001. Inhibition of transforming growth factor-beta signaling accelerates atherosclerosis and induces an unstable plaque phenotype in mice. *Circ. Res.* 89:930–934. doi:10.1161/hh2201.099415

Massagué, J. 1998. TGF-beta signal transduction. *Annu. Rev. Biochem.* 67:753–791. doi:10.1146/annurev.biochem.67.1.753

Massagué, J., S.W. Blain, and R.S. Lo. 2000. TGFbeta signaling in growth control, cancer, and heritable disorders. *Cell.* 103:295–309. doi:10 .1016/S0092-8674(00)00121-5

Schlittenhardt, D., A. Schober, J. Strelau, G.A. Bonaterra, W. Schmiedt, K. Unsicker, J. Metz, and R. Kinscherf. 2004. Involvement of growth differentiation factor-15/macrophage inhibitory cytokine-1 (GDF-15/ MIC-1) in oxLDL-induced apoptosis of human macrophages in vitro and in arteriosclerotic lesions. *Cell Tissue Res.* 318:325–333. doi:10 .1007/s00441-004-0986-3

Shi, Y., and J. Massagué. 2003. Mechanisms of TGF-beta signaling from cell membrane to the nucleus. *Cell.* 113:685–700. doi:10.1016/S0092-8674(03)00432-X

Tacke, F., D. Alvarez, T.J. Kaplan, C. Jakubzick, R. Spanbroek, J. Llodra, A. Garin, J. Liu, M. Mack, N. van Rooijen, et al. 2007. Monocyte subsets differentially employ CCR2, CCR5, and CX3CR1 to accumulate within atherosclerotic plaques. *J. Clin. Invest.* 117:185–194. doi:10.1172/JCI28549

Thorp, E., D. Cui, D.M. Schrijvers, G. Kuriakose, and I. Tabas. 2008. Mertk receptor mutation reduces efferocytosis efficiency and promotes apoptotic cell accumulation and plaque necrosis in atherosclerotic lesions of apoe-/- mice. *Arterioscler. Thromb. Vasc. Biol.* 28:1421–1428. doi:10.1161/ATVBAHA.108.167197

Vergunst, C.E., D.M. Gerlag, L. Lopatinskaya, L. Klareskog, M.D. Smith, F. van den Bosch, H.J. Dinant, Y. Lee, T. Wyant, E.W. Jacobson, et al. 2008. Modulation of CCR2 in rheumatoid arthritis: a double-blind, randomized, placebo-controlled clinical trial. *Arthritis Rheum.* 58:1931–1939. doi:10.1002/art.23591

Vroon, A., C.J. Heijnen, and A. Kavelaars. 2006. GRKs and arrestins: regulators of migration and inflammation. *J. Leukoc. Biol.* 80:1214–1221. doi:10.1189/jlb.0606373

Wollert, K.C., T. Kempf, T. Peter, S. Olofsson, S. James, N. Johnston, B. Lindahl, R. Horn-Wichmann, G. Brabant, M.L. Simoons, et al. 2007. Prognostic value of growth-differentiation factor-15 in patients with non–ST-elevation acute coronary syndrome. *Circulation.* 115:962–971. doi:10.1161/CIRCULATIONAHA.106.650846

Xu, J., T.R. Kimball, J.N. Lorenz, D.A. Brown, A.R. Bauskin, R. Klevitsky, T.E. Hewett, S.N. Breit, and J.D. Molkentin. 2006. GDF15/MIC-1 functions as a protective and antihypertrophic factor released from the myocardium in association with SMAD protein activation. *Circ. Res.* 98:342–350. doi:10.1161/01.RES.0000202804.84885.d0